

Production, Purification, and Characterization of a Mg^{2+} -Responsive Porphobilinogen Synthase from *Pseudomonas aeruginosa*[†]

Nicole Frankenberg,[‡] Dirk W. Heinz,^{‡,§} and Dieter Jahn^{*,‡}

Institut für Organische Chemie und Biochemie, Albert-Ludwigs-Universität, Albertstrasse 21, 79104 Freiburg im Breisgau, Germany, and Abteilung Strukturforschung, Gesellschaft für Biotechnologische Forschung (GBF), Mascheroder Weg 1, 38124 Braunschweig, Germany

Received March 19, 1999; Revised Manuscript Received June 7, 1999

ABSTRACT: During tetrapyrrole biosynthesis the metalloenzyme porphobilinogen synthase (PBGS) catalyzes the condensation of two molecules of 5-aminolevulinic acid to form the pyrrole porphobilinogen. *Pseudomonas aeruginosa* PBGS was synthesized in *Escherichia coli*, and the enzyme was purified as a fusion protein with glutathione *S*-transferase (GST). After removal of GST, a molecular mass of $280\,000 \pm 10\,000$ with a Stokes radius of 57 Å was determined for native PBGS, indicating a homooctameric structure of the enzyme. Mg^{2+} stabilized the oligomeric state but was not essential for octamer formation. Alteration of N-terminal amino acids changed the oligomeric state and reduced the activity of the enzyme, revealing the importance of this region for oligomerization and activity. EDTA treatment severely inhibited enzymatic activity which could be completely restored by the addition of Mg^{2+} or Mn^{2+} . At concentrations in the micromolar range Co^{2+} , Zn^{2+} , and Ni^{2+} partially restored EDTA-inhibited enzymatic activity while higher concentrations of Zn^{2+} inhibited the enzyme. Pb^{2+} , Cd^{2+} , and Hg^{2+} did not restore activity. A stimulatory effect of monovalent ions was observed. A K_m of 0.33 mM for ALA and a maximal specific activity of $60\text{ }\mu\text{mol h}^{-1}\text{ mg}^{-1}$ at the pH optimum of 8.6 in the presence of Mg^{2+} and K^{+} were found. pH-dependent kinetic studies were combined with protein modifications to determine the structural basis of two observed pK_a values of approximately 7.9 (pK_{a1}) and 9.5 (pK_{a2}). These are postulated respectively as ionization of an active site lysine residue and of free substrate during catalysis. Some PBGS inhibitors were characterized. Finally, we succeeded in obtaining well-ordered crystals of *P. aeruginosa* PBGS complexed with the substrate analogue levulinic acid.

Porphobilinogen synthase (PBGS),¹ also known as 5-aminolevulinic acid dehydratase (EC 4.2.1.24) catalyzes the asymmetric condensation of two molecules of 5-aminolevulinic acid (ALA) to form the pyrrole derivative porphobilinogen. This reaction is the first common step in tetrapyrrole biosynthesis and is essential for almost all living organisms to form heme, chlorophyll, cofactor F_{430} , or corrins (1, 2). PBGS's have been successfully purified from a wide variety of sources, and most possess a homooctameric structure (3). During the catalytic process the two substrate molecules of ALA are distinguished by the side chain they contribute to the product porphobilinogen. The one that contributes to the acetate side chain is known as A-side ALA while the one that is involved in propionate side chain formation is named P-side ALA. There is structural and

functional evidence for an initial Schiff base formation between a conserved lysine residue and the P-side ALA molecule (4, 5). Two possible mechanisms for the subsequent formation of porphobilinogen differ mainly in the order of C–C (aldol condensation) and C–N bond formation (Schiff base) (2). All PBGS's which have been purified and characterized to date are metalloenzymes and require either Mg^{2+} , Zn^{2+} , or both for catalysis. Plant enzymes utilize Mg^{2+} , mammalian and yeast enzymes utilize Zn^{2+} , and bacterial enzymes have been shown to utilize either or both metal ions (2, 6–10).

Recently, the structure of the Zn^{2+} -dependent enzyme from yeast was solved (5). The PBGS monomer consists of a TIM barrel with an N-terminal extension involved in the formation of a head-to-tail dimer that further oligomerizes to form the native octamer. The N-terminal extension seems to be important for both dimer and octamer formation. Here we describe the structural characterization and crystallization of a Mg^{2+} -dependent enzyme from the Gram-negative pathogenic bacterium *Pseudomonas aeruginosa*.

MATERIALS AND METHODS

Construction of a *P. aeruginosa* hemB Expression Vector. The complete *P. aeruginosa* hemB gene (11) was amplified from the chromosome via PCR using the primers 5'-GTAAGGCCTGAGCTTCACTCCCGCC-3' and 5'-CGGCG-

[†] This work was supported by the Deutsche Forschungsgemeinschaft (Ja 470/3-4, Ja 470/5-1), Sonderforschungsbereich 388, Albert-Ludwigs-Universität Freiburg, and Fonds der Chemischen Industrie.

* To whom correspondence should be addressed. Tel: +49-761-2036060. Fax: +49-761-2036096. E-mail: jahndiet@uni-freiburg.de.

[‡] Albert-Ludwigs-Universität.

[§] Gesellschaft für Biotechnologische Forschung.

¹ Abbreviations: PBGS, porphobilinogen synthase; ALA, 5-aminolevulinic acid; EDTA, ethylenediaminetetraacetic acid; GST, glutathione *S*-transferase; Na-HEPES, 2-[4-(2-hydroxyethyl)-1-piperazinyl]ethanesulfonic acid sodium salt; IPTG, isopropyl β -D-thiogalactopyranoside; PBS, phosphate-buffered saline; PMSF, phenylmethanesulfonyl fluoride.

GCCGCGATACGTTTCGATCTCAT-3', which contain the underlined *Sma*I and *Not*I sites, respectively. The 1058 bp PCR product was cut with both enzymes and inserted into *Sma*I/*Not*I cut pGEX-6P-1 to create pGEXhemB. The integrity of the constructed plasmid was verified by complete DNA sequence determination of the insert. The constructed vector pGEXhemB contains the *hemB* gene fused downstream from the glutathione *S*-transferase (GST) gene of *Schistosoma japonicum* under the control of a *ptac* promoter. A recognition sequence for PreScission protease, which itself is a fusion of GST with human rhinovirus 3C protease, is located upstream of *hemB*. Proteolytic cleavage yields the native *P. aeruginosa* PBGS with a nine amino acid N-terminal extension.

Complementation of an *Escherichia coli* *hemB* Mutant (RP523) by pGEXhemB. The heme auxotrophic *E. coli* *hemB* mutant RP523 (12) was complemented with the expression vector pGEXhemB as described before (11).

PBGS Synthesis and Purification. pGEXhemB was transformed into *E. coli* BL21(DE3) (13). Bacteria were grown at 37 °C in 500 mL batches of Luria–Bertani media containing ampicillin (100 µg/mL) to an OD_{578nm} of 0.7 and induced by the addition of 1 mM IPTG. Cultures were incubated for an additional 16 h, and bacteria were subsequently harvested by centrifugation at an OD_{578nm} of 7.6. From a total 5 L growth, a bacterial pellet (20 g) was resuspended in 50 mL of phosphate-buffered saline (PBS) containing 1 mM phenylmethanesulfonyl fluoride (PMSF) and disrupted with a French press (3 × 20000 lb/in.²). Cell debris was removed by centrifugation for 45 min at 23000g. The resulting supernatant was directly loaded onto a glutathione–Sepharose 4B column (1 cm × 10 cm) which had been previously equilibrated with 5 column volumes of PBS. Unbound protein was removed by washing the column with 5 column volumes of PBS. GST–PBGS fusion protein was eluted with 50 mM Tris-HCl, pH 8.0, and 10 mM reduced glutathione. GST–PBGS-containing fractions were determined spectroscopically and by SDS–PAGE, pooled, and dialyzed overnight at 4 °C against PreScission protease cleavage buffer (50 mM Tris-HCl, pH 7.0, 150 mM NaCl, 1 mM EDTA, and 1 mM dithiothreitol). Digestion of the fusion protein was performed by addition of two units of PreScission protease for each 100 µg of fusion protein and incubation for 5 h at 4 °C. Removal of uncleaved fusion protein and the excised GST-tag was achieved by loading the digestion mixture onto glutathione–Sepharose 4B. As expected, all recombinant native *P. aeruginosa* PBGS was detected in the flow-through while the protease, the removed GST-tag, and uncleaved GST–PBGS fusion protein remained bound to the column. An additional purification step using MonoQ ion-exchange chromatography was performed to remove residual contaminations and to concentrate the enzyme. A MonoQ HR10/10 column was loaded with up to 25 mg of protein/mL of column volume in 50 mM Na-HEPES, pH 8.0, and 5 mM MgCl₂ (buffer A). Proteins were eluted with a linear gradient of 0–1000 mM KCl in buffer A. For further analysis the enzyme was dialyzed against buffer A. If necessary, the protein solution was concentrated using Centricon-10 concentrator devices to 10 mg/mL. Sterile filtered protein in buffer A is stable up to 6 weeks at 4 °C. All chromatographic procedures were performed on a ÄKTA Explorer system (Pharmacia, Freiburg, Germany).

Determination of Protein Concentration. One absorption unit at 280 nm represents approximately 1.35 mg of PBGS/mL (14).

Gel Permeation Chromatography and Stokes Radius Determination. A Pharmacia Superdex 200 HR16/10 gel filtration column was equilibrated in 50 mM Na-HEPES buffer, pH 7.5, containing 200 mM KCl, 5 mM MgCl₂, and 10% (v/v) glycerol (gel filtration buffer) at a flow rate of 0.4 mL/min. Standards with known *M_r* were applied to the column (300 µg each), and their elution volumes were determined spectroscopically. A sample containing alcohol dehydrogenase as internal standard and *P. aeruginosa* PBGS or GST–PBGS fusion protein were chromatographed under identical conditions. Similar experiments were carried out using gel filtration buffer supplemented with 5 mM EDTA instead of MgCl₂ to determine the involvement of divalent cations in quaternary structure stability. For these experiments the enzyme preparation was preincubated with 5 mM EDTA for 15 min at 37 °C. Estimation of the Stokes radius was performed as per Siegel and Monty (15).

Native Gel Electrophoresis. PBGS (20 µg) in 100 mM bis-tris propane-HCl, 10 mM KCl, and 1 mM MgCl₂ was run with 10 mA on a 12.5% acrylamide gel in the presence and absence of 10 mM EDTA and/or 2 mM ALA, using the PhastGel system of Amersham Pharmacia Biotech.

Sedimentation Coefficient Determination by Glycerol Gradient Centrifugation. PBGS or GST–PBGS (40 µg) was sedimented through a 2.5 mL continuous 10–35% glycerol gradient in gel filtration buffer. The gradient was centrifuged at 100000g at 4 °C for 18 h in a Kontron TST60.4 rotor. After centrifugation 200 µL fractions were collected from the top of the gradient, dialyzed against buffer A, and analyzed for enzymatic activity. In a parallel gradient 30 µg of marker protein with known *M_r* was sedimented under identical conditions, and the fractions obtained were analyzed by SDS–PAGE. The positions of the marker proteins in the gradient were plotted against their known *s*_{20,w} values. The sedimentation coefficients for PBGS and GST–PBGS were interpolated from the standard curve. The approximate native molecular weights for PBGS and the fusion protein were calculated as described by Martin and Ames (16).

Dynamic Light Scattering. The translational diffusion coefficient was measured using a DynaPro-801 detector (Protein Solutions Inc., Charlottesville, VA). Data analysis was performed with the AutoPro software supplied with the DynaPro-801. The enzyme sample (300 µL, 1 mg/mL) in 50 mM Na-HEPES, pH 7.5, 5 mM MgCl₂ and 100 mM KCl was injected into a DynaPro-801 detector through a 0.2 µm filter. The data were collected at 28 °C, and 60 measurements were averaged for the final statistics. The hydrodynamic radius was estimated using the Stokes–Einstein equation $R_H = kT/6\pi\eta D_T$, where *k* is Boltzmann's constant and the viscosity η was estimated to be 1.019 cP. The molecular weight was estimated from an empirical relationship between *R_H* and molecular weight using bovine serum albumin as a standard.

Isoelectric Focusing. Isoelectric focusing of PBGS was performed on Servalyt Precote gels (pH 3–10) using a Pharmacia Multiphor apparatus. Protein samples (20 µg) were applied to the gel (125 mm × 125 mm) and electro-focused for 2 h at 4 W. Proteins were detected by Coomassie

brilliant blue staining. Protein standards with known *pI* values were employed for calibration.

N-Terminal Sequencing by Edman Degradation. PBGS (20 μg) was sequenced using an Applied Biosystems 477A sequencer linked to a 120A analyzer.

Electrospray Ionization Mass Spectrometry (ESI-MS). Electrospray ionization mass spectrometry data were collected using a Finnigan Mat TSQ 7000 spectrometer. The analysis was carried out with 50 μL of PBGS (1 mg/mL) in 30% methanol containing 0.01% acetic acid.

PBGS Activity Assay. PBGS activity was determined by the amount of porphobilinogen formed from ALA. For this purpose a modified Ehrlich test was performed. For standard tests 2 μg of enzyme was incubated in a total volume of 250 μL buffer A. The enzymatic reaction was started by the addition of ALA (5 mM final concentration) prepared in 50 mM Na-HEPES, pH 8.0. The assay mixture was incubated at 37 °C for 15 min. The reaction was terminated by the addition of 25 μL of 50% (w/v) trichloroacetic acid at 4 °C for 15 min. The mixture was centrifuged for 10 min at 15 000 rpm in a tabletop centrifuge at 4 °C, and the clear supernatant was reacted with an equal volume of Ehrlich's reagent (17). After 15 min of color development the absorbance at 555 nm was measured. A molar extinction coefficient for porphobilinogen of 60 200 $\text{M}^{-1} \text{cm}^{-1}$ was used to calculate the porphobilinogen concentration. One unit of enzymatic activity corresponds to 1 μmol of porphobilinogen formed h^{-1} (mg of protein) $^{-1}$ at 37 °C.

Crystallization of PBGS. Crystals of PBGS were grown using the hanging-drop vapor diffusion method. Initial crystallization setups were performed by using a multifactorial screening kit containing a total of 98 different buffered precipitant solutions (Hampton Research, Laguna Hills, CA) at 4 and 20 °C. A freshly prepared PBGS solution (5 μL , 6–12 mg/mL) in 20 mM Na-HEPES buffer, pH 8.0, containing 10 mM MgCl_2 , which was previously incubated with 10 mM substrate analogue levulinic acid was mixed on a cover slide with an equal amount of precipitant solution and mounted above a 500 μL reservoir of precipitant solution. Small squared plates appeared after 3–7 days under a variety of conditions.

Generation of Apo-PBGS and Analysis of Metal Dependence. PBGS (1 mg/mL) was incubated with 5 mM EDTA for 15 min at 37 °C followed by overnight dialysis against 50 mM Na-HEPES, pH 8.0. The resulting PBGS had a residual activity of ~4% and is defined as apo-PBGS. For metal activation experiments apo-PBGS was incubated for 15 min with indicated concentrations of different divalent cations in assay buffer; subsequently, ALA was added and the protein assayed for PBGS activity. Metal titration experiments were also carried out with apo-PBGS. Apoenzyme was incubated with the two metals (Zn^{2+} and Mg^{2+}) at different indicated concentrations for 15 min prior to substrate addition. The influence of monovalent cations was tested in 100 mM bis-tris propane-HCl, pH 6.9, with a full complement of MgCl_2 (10 mM) and in the presence of given concentrations of KCl, NaCl, NH_4Cl , and LiCl. Other buffer systems such as Na-HEPES were avoided due to the requirement of monovalent cations in pH adjustment.

pH-Dependent Kinetics and Chemical Protein Modification. A range of 100 mM bis-tris propane-HCl buffers within the pH range of 6.6–10.2 varying by 0.2 pH unit were

prepared, and the kinetic measurements were performed. All buffers contained 100 mM KCl and 5 mM MgCl_2 . A range of substrate concentrations between 0.05 and 10 mM ALA were prepared and used in the same buffer. The results obtained were checked for adherence to Michaelis–Menten kinetics.

For chemical modification reactions targeting histidine and lysine residues 2 μg of enzyme was incubated with different concentrations of modifying reagent for various times (5–60 min). ALA was subsequently added to a final concentration of 5 mM, and enzymatic activity was assayed in the mixture containing the inactivating reagents described above. PBGS modifications were carried out using pyridoxal 5'-phosphate prepared in aqueous solution (0–1 mM final concentration) for the modification of lysine residues. Schiff base formation of pyridoxal 5'-phosphate with active site lysine residues was followed spectroscopically. Diethyl pyrocarbonate prepared in ethanol (0–100 mM final concentration) was used for the modification of histidine residues. Modification reactions with diethyl pyrocarbonate were carried out in phosphate buffer at pH 6.2. Additions of 20 mM imidazole terminated the reaction and adjusted the pH to 8.0. PBGS activity was assayed as described above. All buffers employed contained both magnesium and monovalent cations.

Inhibition Studies. Potential PBGS inhibitors (levulinic acid, succinic acid, succinic acid monomethyl ester, 2,2-difluorosuccinic acid, and protoporphyrin IX) were studied for their capacity to inhibit *P. aeruginosa* PBGS. For this purpose 2 μg of enzyme was incubated with a range of inhibitor concentrations for 30 min at room temperature in buffer A. ALA was added to a final concentration of 5 mM. Two inhibitor concentrations were selected, and time-dependent kinetics with different ALA concentrations were performed. Lineweaver–Burke plots were used to determine the type of inhibition. The inhibitor constant K_i reflecting the concentration that gave 50% inhibition was determined by Dixon plot (18).

RESULTS AND DISCUSSION

Synthesis, Purification, and Initial Characterization of *P. aeruginosa* PBGS. *P. aeruginosa* PBGS was synthesized as a fusion protein with GST in *E. coli* and purified by affinity chromatography as described in Materials and Methods. The GST-tag was removed via site-specific protease digestion. A second affinity chromatography yielded protein at >90% homogeneity which could be further purified to apparent homogeneity by ion-exchange chromatography. Figure 1 shows an SDS–PAGE of the purification and processing of the protein. One liter of bacterial culture yielded about 10 mg of recombinant PBGS with a specific activity of 60 μmol of porphobilinogen formed h^{-1} (mg of protein) $^{-1}$ (60 units/mg) and an apparent K_m value for ALA of 0.33 mM at pH 8.6 in Na-Hepes. This specific activity is comparable to that of other purified bacterial PBGS (6, 10, 12). The molecular weight for a monomer of *P. aeruginosa* PBGS deduced from the *hemB* gene sequence is 37 008. However, the cloning and expression strategy for the *hemB* gene using pGEX-6-P1 was responsible for an additional nine N-terminal amino acids after protease treatment. During this process, the first amino acid encoded by the *hemB* was altered to leucine.

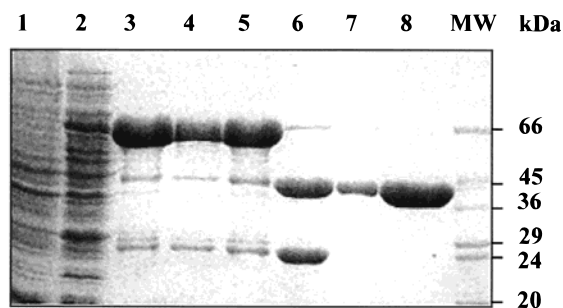


FIGURE 1: SDS-PAGE of the purification and processing of recombinant *P. aeruginosa* PBGS. Lanes 1, cell-free extract from uninduced *E. coli* BL21(DE3) carrying pGEXhemB; 2, cell-free extract from IPTG-induced *E. coli* BL21(DE3) carrying pGEXhemB; 3–5, GST–PBGS-containing fractions after glutathione–Sepharose affinity chromatography; 6, GST–PBGS after PreScission protease treatment; 7, purified recombinant PBGS after a second glutathione–Sepharose affinity chromatography; 8, PBGS after final purification by MonoQ ion-exchange chromatography; MW, dalton marker.

Therefore, the calculated subunit molecular weight for the recombinant protein is 37 832. The N-terminal sequence of the purified enzyme was confirmed by Edman degradation. The first 20 amino acids were found to be GPLGSPEFP L S-FTPANRAYP, which is in agreement with the protein sequence deduced from the gene and vector sequence (8). The subunit molecular weight was experimentally confirmed by electrospray ionization mass spectrometry.

To measure *in vivo* activity of the GST–PBGS fusion protein transformation of a heme auxotrophic *E. coli* *hemB* mutant (RP523) with the GST–PBGS fusion protein encoding plasmid was performed. The *hemB* mutant was efficiently complemented to heme prototrophy in the presence of IPTG. The control plasmid pGEX failed to complement the *hemB* mutant. The presence of the fusion protein in the mutant was verified by SDS–PAGE. In agreement with these findings, the *in vitro* activity of the fusion protein after purification was about 25% of the native PBGS (specific activity of the fusion protein was determined with an appropriate correction for the molecular mass of the fusion protein).

Determination of Native Molecular Mass and Isoelectric Point. All studied Zn^{2+} -dependent PBGS are reported to be octamers (2, 3). However, there are conflicting reports about the quaternary structure of Mg^{2+} -dependent PBGS's. Some plant enzymes are reported to be hexameric (spinach, *Scenedesmus oliquus*); others are reported to be octamers (pea) (7, 19–21). Only a few Mg^{2+} -dependent bacterial PBGSs have been purified and studied so far. The enzyme of *Bradyrhizobium japonicum* has an octameric structure (10). Therefore, we very carefully analyzed the quaternary structure of the *P. aeruginosa* enzyme. Three independent methods, gel permeation chromatography using the molecular sieving matrix Superdex 200, rate zonal sedimentation in a glycerol gradient, and dynamic light scattering, were used to determine the relative molecular mass of the native enzyme. Gel permeation chromatography was performed as described in Materials and Methods. After prec calibration of the column with the marker proteins PBGS was chromatographed and localized using activity testing as well as SDS–PAGE (Figure 2A). Known Stokes radii of the marker proteins used for Superdex 200 column calibration were plotted versus their $-(\log K_{av})^{1/2}$ (see Figure 2B), where K_{av}

$= (V_e - V_0)/(V_t - V_0)$. V_e is the elution volume of each protein, V_0 is the column void volume, and V_t corresponds to the total column volume. PBGS eluted with a V_e of 12 mL on a 23 mL Superdex 200 column which by comparison to the calibration run revealed a relative molecular mass of $280\,000 \pm 10\,000$ (Figure 2A,B). Alcohol dehydrogenase was used as an internal standard to allow precise molecular mass determination. A Stokes radius of 57 Å was obtained (Figure 2B), indicating the largest dimensions of the PBGS protein to be about 114 Å. For the rate zonal sedimentation analysis, the peak of PBGS activity was located between the two marker proteins catalase (250 000) and urease (493 000) of the parallel marker run as shown in Figure 2C. The majority of PBGS protein was detected in the corresponding fractions using SDS–PAGE. A sedimentation coefficient $s_{20,w}$ of 11×10^{-13} s for PBGS was deduced from a standard plot of the known $s_{20,w}$ values of different marker proteins (Figure 2D). A native molecular mass of $280\,000 \pm 10\,000$ was calculated for PBGS using the relationship between the sedimentation coefficient of a protein and its molecular mass (16). The hydrodynamic radius of PBGS determined using the Stokes–Einstein equation for the results from dynamic light scattering was 58 Å. The deduced molecular mass then confirmed the results obtained by the other two methods. On the basis of these experiments we conclude that *P. aeruginosa* PBGS is an octameric protein of approximately 300 000 Da, which is in good agreement with most other known PBGS's and is consistent with the crystal structure of the yeast enzyme (5). Isoelectric focusing of *P. aeruginosa* PBGS gave a single major band corresponding to a *pI* of 5.4. This is about the same value as that obtained for the Mg^{2+} -dependent pea enzyme (21) and matches approximately the calculated value of 4.97 (DNAS tar Protean, DNAS tar Inc., 1990–1994).

Influence of EDTA Treatment on the Oligomeric State. To study the role of Mg^{2+} in the quaternary structure of *P. aeruginosa* PBGS, gel permeation chromatography, glycerol gradient centrifugation, and native gel electrophoresis were performed using apoprotein in the presence of EDTA. Incubation of *P. aeruginosa* PBGS with EDTA resulted in the dramatic reduction of activity (see below). Generation of apo-PBGS by incubation of enzyme with 5 mM EDTA followed by gel permeation chromatography in the presence of 5 mM EDTA did not change the elution profile on the Superdex 200 column compared to untreated enzyme. After addition of MgCl_2 to the PBGS-containing fractions ($V_e = 12$ mL) full enzyme activity was retained. After glycerol gradient centrifugation in the presence of 5 mM EDTA PBGS activity was again detected after MgCl_2 addition in fraction 10. No other fractions of the gel permeation chromatography run and the glycerol gradient contained active or inactive PBGS protein as determined by SDS–PAGE. These results suggest that the removed metal ions are important for activity (see below) but their removal does not compromise the quaternary structure once it is formed. However, native gel electrophoresis promotes the dissociation of EDTA-treated PBGS as was seen previously for *E. coli* PBGS (22). The metal-free *P. aeruginosa* PBGS, while stable under mild analytical conditions (gel permeation chromatography), loses its oligomeric integrity in the electric field during native gel electrophoresis. From these experiments we conclude that Mg^{2+} is not essential for octamer formation

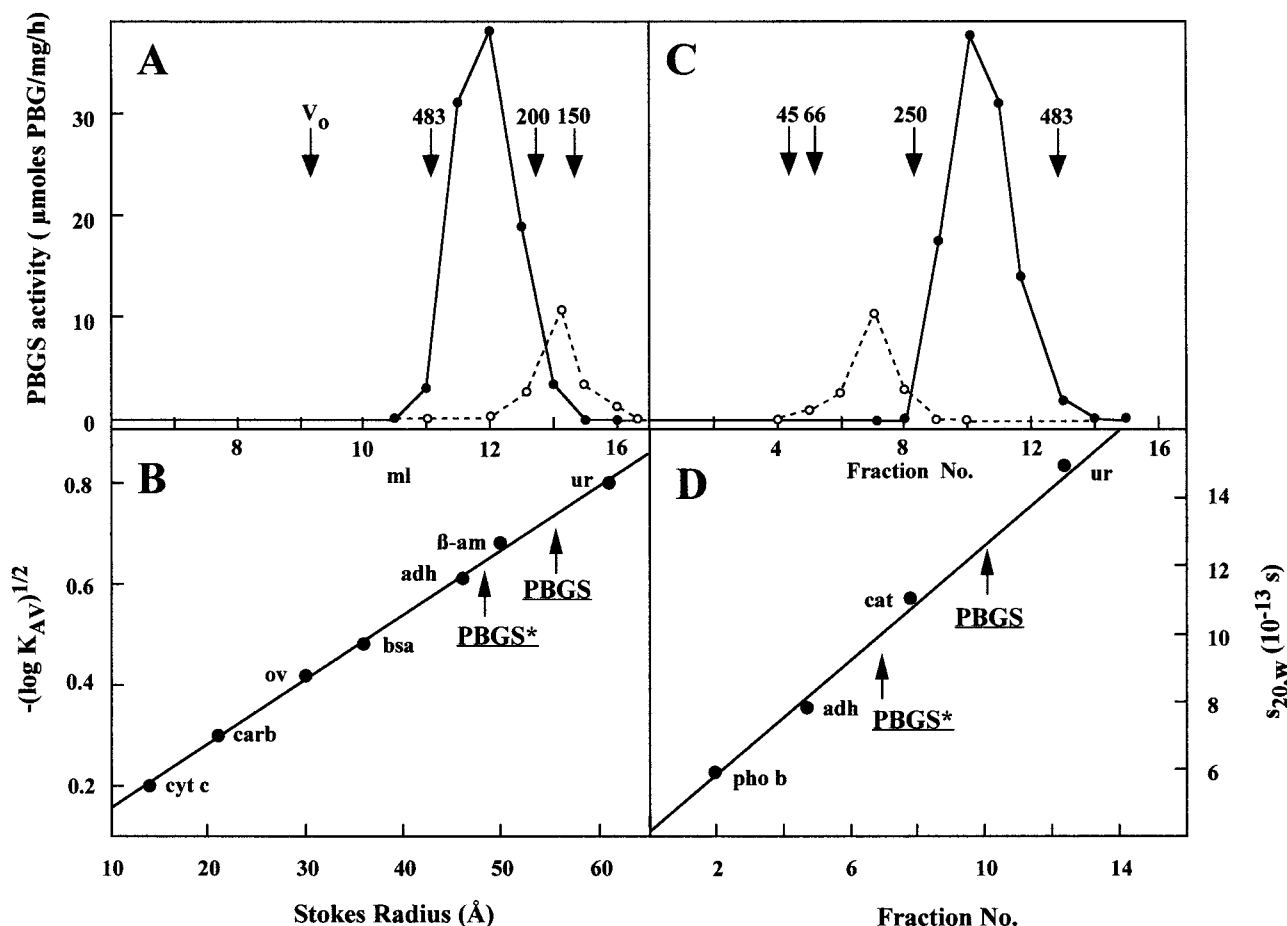


FIGURE 2: Estimation of the native molecular mass by gel permeation chromatography and glycerol gradient centrifugation and calculation of the Stokes radius and sedimentation coefficient of PBGS (●) and PBGS* (○). (A) PBGS and PBGS* (GST–PBGS fusion protein) were chromatographed through a Superdex 200 column which had been precalibrated with the following marker proteins: urease (ur) (483 kDa), β -amylase (β -am) (200 kDa), alcohol dehydrogenase (adh) (150 kDa), bovine serum albumin (bsa) (66 kDa), ovalbumin (ov) (45 kDa), carbonic anhydrase (carb) (29 kDa), and cytochrome *c* (cyt *c*) (12.4 kDa). An aliquot of each fraction was assayed for PBGS activity. (B) Estimation of the Stokes radius of PBGS and PBGS*. (C) Estimation of the molecular mass by sedimentation through glycerol gradients. Marker proteins phosphorylase *b* (pho *b*) (97 kDa), alcohol dehydrogenase (adh) (150 kDa), catalase (cat) (250 kDa), and urease (ur) (483 kDa) were sedimented through a parallel gradient. (D) Estimation of the sedimentation coefficient of PBGS and PBGS*.

but stabilizes the oligomeric state of the enzyme. The *E. coli* PBGS octamer was found to dissociate during native gel electrophoresis; EDTA enhanced the dissociation and Mg^{2+} and/or ALA prevented the dissociation (22). Contrary to what was seen with *E. coli* PBGS, the substrate ALA does not enhance the octameric stability of *P. aeruginosa* PBGS during electrophoresis.

The N-Terminal Part of PBGS Is Important for Oligomerization and Activity. The crystal structure of Zn^{2+} -dependent yeast PBGS indicated the importance of the N-terminus in both dimer and octamer stability (5). Four dimers are seen to form the octamer with the N-terminal arm as central to monomer–monomer interactions. Two observations allowed a functional evaluation of the importance of the N-terminus in oligomerization of the *P. aeruginosa* enzyme. For the complete fusion protein of GST N-terminally fused to PBGS, gel permeation chromatography experiments showed a salt concentration dependence of the oligomerization states. Under the conditions employed for native PBGS (200 mM KCl) most of the GST–PBGS fusion protein was found in the exclusion volume as a large aggregate. Only at salt concentrations above 500 mM KCl was the fusion protein able to form active octamers. N-Terminally fused GST prevented stable oligomer forma-

tion of PBGS, leading to the observed unspecific aggregation of proteins. High ionic strength abolished aggregation by competition for unspecific ionic interactions or by an increase of specific hydrophobic interactions. Following cleavage of the GST, no aggregation of *P. aeruginosa* PBGS was observed regardless of the ionic strength.

Further evidence for the importance of the N-terminal region for quaternary structure formation and stability came for a serendipitous mutant. In this case PBGS carrying a mutation leading to an exchange of the first N-terminal amino acids of the original PBGS sequence from VSFTPANRAY-PYTRLRR to VSLLPPIAPIPTPRLRR revealed a tetrameric structure in glycerol gradient centrifugation and gel permeation chromatography experiments (PBGS* in Figure 2). The experiments outlined indicated the importance of the N-terminus for oligomerization, oligomer stability, and enzyme activity.

Divalent Metal Requirement of *P. aeruginosa* PBGS. For an initial characterization of metal ion requirement, we incubated the enzyme with the chelator EDTA, which resulted in the immediate and dramatic reduction in activity. Even extensive dialysis against metal-free buffer was able to drastically reduce enzyme activity, thus indicating a loosely bound metal ion. After dialysis to remove EDTA

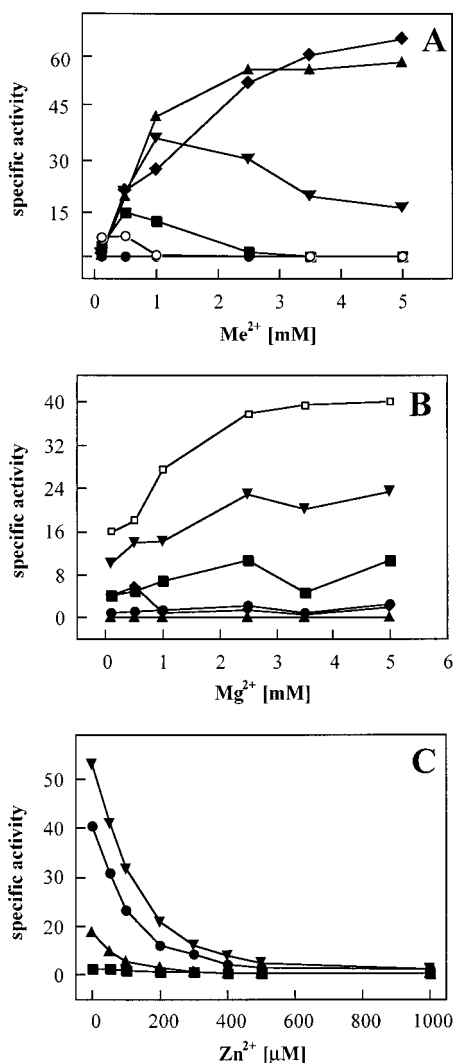


FIGURE 3: Metal dependence of PBGS. (A) Ability of different divalent cations to restore activity of apo-PBGS: (◆) $MgCl_2$, (▲) $MnCl_2$, (▼) $CoCl_2$, (■) $NiCl_2$, (○) $ZnCl_2$, and (●) $HgCl_2$, $CdCl_2$, and $PbNO_3$. (B) $MgCl_2$ activation of apo-PBGS with increasing $MgCl_2$ concentrations at fixed Zn^{2+} concentration: (□) 50 μ M, (▼) 100 μ M, (■) 200 μ M, (●) 300 μ M, (◆) 400 μ M, and (▲) 500 μ M. (C) PBGS specific activity as a function of $ZnCl_2$ in the assay. For each curve, the concentration of $ZnCl_2$ was varied from 0 to 1000 μ M, and the concentration of $MgCl_2$ was fixed at 10 mM (▼), 5 mM (●), 1 mM (▲), and 100 mM (■).

we tested the ability of various divalent cations to restore PBGS activity (Figure 3A). Mg^{2+} and Mn^{2+} restored activity up to 100%. Co^{2+} and Ni^{2+} sustained PBGS activity to approximately 50% and Zn^{2+} only to 10%. Zn^{2+} concentrations, even in the micromolar range, had an inhibitory effect on the enzyme (Figure 3A,B). The heavy metal ions Cd^{2+} , Pb^{2+} , and Hg^{2+} did not reactivate the EDTA-inhibited enzyme. Incubation of the enzyme at constant Mg^{2+} concentration with increasing Zn^{2+} concentration led to the complete loss of activity (Figure 3B). In the reverse experiment increasing Mg^{2+} concentration yielded an increase of PBGS activity (Figure 3C). However, at high concentrations of Zn^{2+} , Mg^{2+} was not able to overcome the toxic effect of Zn^{2+} and the enzyme remained inhibited. These experiments identify *P. aeruginosa* PBGS as a Mg^{2+} metalloenzyme but do not establish the number of different Mg^{2+} sites nor the total Mg^{2+} stoichiometry (23). To date, two different roles have been determined for Mg^{2+} in PBGS

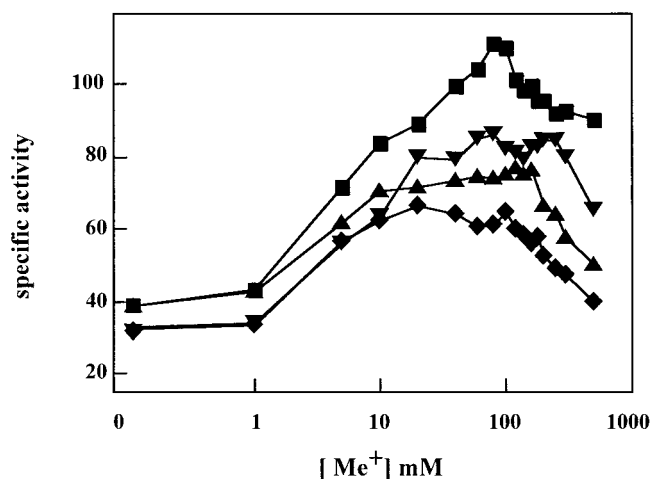


FIGURE 4: Influence of monovalent cations on *P. aeruginosa* PBGS activity. The effect of increasing concentrations of KCl (■), NH_4Cl (▼), NaCl (▲), and LiCl (◆) in 100 mM bis-tris propane-HCl pH 6.9 is shown.

(10), and three different roles for divalent metal ions have been proposed (2).

Effect of Monovalent Ions on the Activity of *P. aeruginosa* PBGS. It has been reported that monovalent cations have a stimulatory effect on some PBGS activities (10, 24). The effects observed were seen to be dependent on the buffer system employed because the buffers varied in monovalent cation concentration. A dramatic effect of monovalent cations on *P. aeruginosa* PBGS activity was observed in the buffer bis-tris propane-HCl at pH 6.9 using potassium, sodium, lithium, and ammonium sulfate salts (Figure 4). This phenomenon mirrors that reported for the closely related *B. japonicum* PBGS (10).

Identification of Ionizing Groups during Catalysis Using pH-Dependent Kinetics. The influence of pH on the catalytic parameters of PBGS was determined to obtain information regarding the role of acid-base groups of the enzyme in catalysis. The broad pH spectrum buffer bis-tris propane was used with KCl and Mg^{2+} to control for both anion and cation effects. A plot of k_{cat}/K_m as a function of pH should document the essential ionizing groups of the free enzyme involved in both substrate binding and catalytic processing (25). Figure 5 shows the effect of pH on k_{cat}/K_m of *P. aeruginosa* PBGS. The results were fitted to eq 1, which represents a classical

$$y = \frac{y_{max}}{(10^{-pH}/10^{-pK_{a1}}) + (10^{-pK_{a2}}/10^{-pH}) + 1} \quad (1)$$

bell-shaped curve (25). Although the data do not allow for precise determination of pK_a values, the apparent pK_a values under these conditions are 7.9 for pK_{a1} and 9.5 for pK_{a2} . These pK_a values may vary with the concentration of monovalent and divalent cations as was the case for the near neutral pK_a of the related *B. japonicum* PBGS (10).

To obtain additional evidence for the involvement of ionizing groups in catalysis, reagents for the specific modification of histidine and lysine residues of PBGS were employed. Cysteine-modifying reagents were not used since *P. aeruginosa* PBGS does not possess any cysteine residues. Similar pK_{a1} values between 7.5 and 8.4 have been assigned to cysteinyl residues found in the pea and *E. coli* enzymes (25), but this cannot be the case for *P. aeruginosa* PBGS.

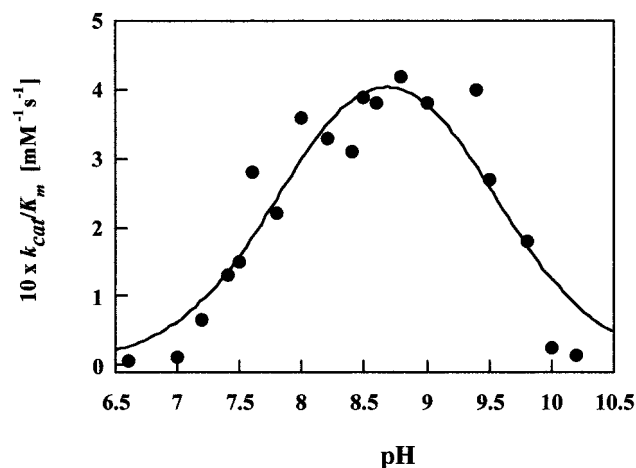


FIGURE 5: Effect of pH on k_{cat}/K_m . The line represents the best fit to eq 1. The approximate value of pK_{a1} is 7.9 and the approximate value of pK_{a2} is 9.5.

P. aeruginosa PBGS was inhibited by diethyl pyrocarbonate ($K_i = 30 \mu\text{M}$), which is known to react with histidine residues. One might be tempted to attribute pK_{a1} to a histidyl involved in catalysis. Histidine residues have been reported before to be involved in PBGS catalysis (26, 27). To determine the role of the only two highly conserved histidine residues of the *E. coli* PBGS, both were mutated (28). It was demonstrated that these histidines residues, of which only one is conserved in the *P. aeruginosa* enzyme (His 136), are not essential to catalysis (28) even though the *E. coli* PBGS was also found sensitive to protein modification by diethyl pyrocarbonate (25). Therefore, the pK_{a1} of 7.9 for the free enzyme might rather reflect the deprotonation of the amino group of free substrate.

Pyridoxal phosphate also inhibited the enzyme in that it forms a Schiff base with reactive, deprotonated lysine residues ($K_i = 30 \mu\text{M}$). The Schiff base formed between pyridoxal phosphate and the enzyme was confirmed by the typical absorbance pattern of the pyridoxal phosphate–enzyme complex (data not shown). Thus, we propose that a pK_{a2} of 9.5 should be assigned to a lysine residue involved in catalysis. A possible candidate is the conserved Lys260 involved in Schiff base formation with P-side ALA.

Inhibitor Studies. *P. aeruginosa* is a widespread pathogen which is involved in numerous human infections and is also known to be resistant to a wide variety of antibiotics. Because the *P. aeruginosa* PBGS represents a Mg^{2+} -dependent enzyme and humans possess a Zn^{2+} -dependent PBGS, inhibitors which solely inhibit the Mg^{2+} -dependent enzyme could provide the basis for the development of new types of inhibitors with potential antibiotic effect. We evaluated some inhibitors with the *P. aeruginosa* enzyme which were previously identified to inhibit other PBGS's. The competitive inhibitory effect of levulinic acid could be confirmed for the *P. aeruginosa* PBGS with a K_i value of 1.5 mM. Succinic acid and its derivatives 2,2-difluorosuccinic acid and succinic acid monomethyl ester also inhibited the enzyme. While succinic acid missing the carbonyl moiety which is important for Schiff base formation in the active site showed noncompetitive inhibition ($K_i = 9 \text{ mM}$), succinic acid monomethyl ester and 2,2-difluorosuccinic acid employed competitive inhibition with K_i values of 1.9 and 7.0 mM, respectively. In general, one could observe that inhibi-

tors of *P. aeruginosa* PBGS all contain a succinyl moiety as well as a carbonyl group possibly important for initial Schiff base formation. Determination of the atomic structure of the Mg^{2+} -dependent enzyme from *P. aeruginosa* will greatly facilitate our attempts to design inhibitors with specificity for Mg^{2+} -dependent PBGS.

Protoporphyrin IX was also shown to inhibit *P. aeruginosa* PBGS with a K_i of $2.5 \mu\text{M}$. Although feedback inhibition of PBGS by protoporphyrin has been proposed (25, 29), the results obtained should to be interpreted with caution. In the micromolar range iron protoporphyrin inhibited in vitro experiments a whole range of different enzymes including RNA polymerases and restriction enzymes (30).

Preliminary Analysis of Crystals of *P. aeruginosa* PBGS. To elucidate the structure of a Mg^{2+} -dependent PBGS at atomic resolution, we performed crystallization experiments using *P. aeruginosa* PBGS. Small squared plates appeared after 3–7 days under various crystallization conditions. The best crystals were obtained using 1.2 M $(\text{NH}_4)_2\text{SO}_4$, 100 mM Tris-HCl, pH 8.5, 12% glycerol, and a protein concentration of 10 mg/mL at 4°C in the presence of the competitive inhibitor levulinic acid at 10 mM. The size of these crystals could be significantly improved (approximately $300 \times 300 \times 50 \mu\text{m}$) by using 3% 2-propanol or 3% glucose as additive. A data set to 2.6 \AA resolution was collected using monochromatic Cu K α radiation generated by a Rigaku RU 200 rotating anode at 4.8 kW and a Nicolet-Siemens X1000 area detector. The crystals belonged to the space group $P4_212$ with cell dimensions of $a = b = 129.8 \text{ \AA}$ and $c = 86.7 \text{ \AA}$. Under the assumption of two molecules (37 kDa) in the asymmetric unit, a V_M value of $2.46 \text{ \AA}^3/\text{Da}$, corresponding to a solvent content of 50% (31), was calculated.

Crystal Structure of the *P. aeruginosa* PBGS. During the reviewing process the crystal structure of *P. aeruginosa* PBGS in complex with levulinic acid (LA) was solved at a resolution of 1.67 \AA (32). The enzyme is an octamer consisting of four asymmetric dimers. Dimer formation is mediated by the N-terminal arm of each monomer. Only one well-defined Mg^{2+} per PBGS dimer was detected. The Mg^{2+} is located approximately 10 \AA away from the metal-free active site with indirect contact to the N-terminal arm of the other monomer. LA is attached via a Schiff base to an active site lysine residue in each monomer. No histidine residues were located in the active site.

CONCLUSION

Recombinant *P. aeruginosa* PBGS is a Mg^{2+} -responsive homooctameric enzyme of $280\,000 \pm 10\,000 \text{ Da}$ with a Stokes radius of 57 \AA . The N-terminal arm of each monomer is important for the formation of the Mg^{2+} -stabilized oligomeric state. The enzyme contains an ionizing active site lysine residue and is stimulated by monovalent cations. The diffracting PBGS crystals obtained provided the basis for structure determination. The accompanying paper elucidates metal ion stoichiometry and functionally identifies *P. aeruginosa* PBGS as a novel type V protein (23).

ACKNOWLEDGMENT

We thank Dr. E. Schiltz for carrying out the Edman sequencing, C. Warth for the electrospray ionization mass spectrometry, and A. Lenhard for help with dynamic light

scattering. We are also thankful to Dr. M. Warren and J. Moser for helpful discussion and to Dr. A. Rompf and Dr. T. Hoffmann for helpful advice in molecular cloning. We thank Dr. E. K. Jaffe for helpful advice on the monovalent cation activation and native gel electrophoresis experiments and for some guidance in preparation of the manuscript. We thank A. Espin for technical assistance and Professor G. E. Schulz for support.

REFERENCES

1. Jahn, D., Hungerer, C., and Troup, B. (1996) *Naturwissenschaften* 83, 389–400.
2. Jaffe, E. K. (1995) *J. Bioenerg. Biomembr.* 27, 169–179.
3. Jordan, P. M. (1991) Biosynthesis of Tetrapyrroles, *New Compr. Biochem.* 19, 1–66.
4. Gibbs, P. N. B., and Jordan, P. M. (1986) *Biochem. J.* 236, 447–451.
5. Erskine, P. T., Senior, N., Awan, S., Lambert, R., Lewis, G., Tickle, I. J., Sarwar, M., Spencer, P., Thomas, P., Warren M. J., Shoolingin-Jordan, P. M., Wood, S. P., and Cooper, J. B. (1997) *Nat. Struct. Biol.* 4, 1025–1031.
6. Bevan, D. R., Bodlaender, P., and Shemin, D. (1980) *J. Biol. Chem.* 255, 2030–2035.
7. Boese, Q. F., Spano, A. J., Li, J. M., and Timko, M. P. (1991) *J. Biol. Chem.* 266, 17060–17066.
8. Mitchell, L. W., and Jaffe, E. K. (1993) *Arch. Biochem. Biophys.* 300, 169–177.
9. Spencer, P., and Jordan, P. M. (1993) *Biochem. J.* 290, 279–287.
10. Petrovich, R. M., Litwin, A., and Jaffe, E. K. (1996) *J. Biol. Chem.* 271, 8692–8699.
11. Frankenberg, N., Kittel, T., Hungerer, C., Römling, U., and Jahn, D. (1998) *Mol. Gen. Genet.* 257, 485–489.
12. Li, J. M., Umanoff, R., Proenca, C., and Cosloy, S. D. (1988) *J. Bacteriol.* 170, 1021–1025.
13. Studier, F. W., Rosenberg, A. H., Dunn, J. J., and Dubendorff, J. W. (1990) *Methods Enzymol.* 185, 60–89.
14. Gill, S. C., and von Hippel, P. H. (1989) *Anal. Biochem.* 182, 319–326.
15. Siegel, L. M., and Monthy K. J. (1966) *Biochim. Biophys. Acta* 112, 346–362.
16. Martin, R. G., and Ames, B. N. (1961) *J. Biol. Chem.* 236, 1372–1379.
17. Mauzerall, D., and Granick, S. (1956) *J. Biol. Chem.* 216, 435–446.
18. Palmer, T. (1985) *Understanding Enzymes*, Wiley, New York.
19. Liedgens, W., Lütz, C., and Schneider, H. A. W. (1983) *Eur. J. Biochem.* 135, 75–79.
20. Stolz, M., and Dörnemann, D. (1996) *Eur. J. Biochem.* 236, 600–608.
21. Cheung, K., Spencer, P., Timko, M. P., and Shoolingin-Jordan, P. M. (1997) *Biochemistry* 36, 1148–1156.
22. Jaffe, E. K., Ali, A., Mitchell, L. W., Taylor, K. T., Volin, M., and Markham, G. D. (1995) *Biochemistry* 34, 244–251.
23. Frankenberg, N., Jahn, D., and Jaffe, E. K. (1999) *Biochemistry* 38, 13976–13982.
24. Nandi, D. L., and Shemin, D. (1968) *J. Biol. Chem.* 243, 1224–1235.
25. Senior, N. M., Brocklehurst, K., Cooper, J. B., Wood, S. P., Erskine, P., Shoolingin-Jordan, P. M., Thomas, P. G., and Warren, M. J. (1996) *Biochem. J.* 320, 401–412.
26. Fukuda, H., Sopenade Kracoff, U. E., Inigo, L. E., Paerdes, S. R., Ferramola de Sancovich, A. M., Sancovich, H. A., and Batlle, A. M. (1990) *J. Enzyme Inhib.* 3, 295–302.
27. Tsukamoto, I., Yoshinaga, T., and Sano, S. (1975) *Biochem. Biophys. Res. Commun.* 67, 294–300.
28. Mitchell, L. W., Volin, M., and Jaffe, E. K. (1995) *J. Biol. Chem.* 270, 24054–24059.
29. Chandrika, S. R., Kumar, C. C., and Padmanaban, G. (1980) *Biochim. Biophys. Acta* 607, 331–338.
30. Haile, J. D., Rouault, T. A., Harford, J. B., and Klausner, R. D. (1990) *J. Biol. Chem.* 265, 12786–12789.
31. Matthews, B. W. (1968) *J. Mol. Biol.* 33, 491–497.
32. Frankenberg, N., Erskine, P. T., Cooper, J. B., Shoolingin-Jordan, P. M., Jahn, D., and Heinz, D. W. (1999) High-resolution crystal structure of a Mg^{2+} -dependent porphobilinogen synthase, *J. Mol. Biol.* 289, 591–602.

BI9906468